Optical properties of ZnO deposited by atomic layer deposition (ALD) on Si nanowires

Viktoriia Fedorenko, Roman Viter, Igor Iatsunskyi, Grzegorz Nowaczyk, Octavio Graniel, Karol Załęski, Stefan Jurga, Valentyn Smyntyna, Philippe Miele, Arunas Ramanavicius, et al.

Optical properties of ZnO deposited by atomic layer deposition (ALD) on Si nanowires

Viktoriia Fedorenko,[1,2] Roman Viter,[3,4] Igor Iatsunskyi,[5]* Grzegorz Nowaczyk,[5] Octavio Graniel,[1] Karol Załęski,[5] Stefan Jurga,[5] Valentyn Smyntyna,[2] Philippe Miele,[1] Arunas Ramanavicius,[6] Sebastien Balme,[1] Mikhael Bechelany[1]**

[1] *Institut Européen des Membranes, UMR 5635, ENSCM, UM, CNRS, Université Montpellier, Place Eugene Bataillon, F-34095 Montpellier cedex 5, France*

[2] *Faculty of Physics, Experimental physics department, Odessa National I.I. Mechnikov University, 42, Pastera, 65026, Odessa, Ukraine*

[3] *Institute of Atomic Physics and Spectroscopy, University of Latvia, 19, Raina Blvd., LV 1586, Riga, Latvia*

[4]*State Research Institute Center for Physical Sciences and Technology, Savanoriuave. 231, LT-01108 Vilnius, Lithuania*

[5] *NanoBioMedical Centre, Adam Mickiewicz University, 85 Umultowska str., 61-614, Poznan, Poland*

[6] *Faculty of Electronics, Vilnius Gediminas Technical University, Sauletekio 11, LT-10223 Vilnius, Lithuania*

* *Corresponding author: roman.viter@lu.lv, Phone: +37120058754*

* *Corresponding author: yatsunskiy@gmail.com, Phone: +48731308173*

* *Corresponding author: mikhael.bechelany@umontpellier.fr, Phone: +33467149167, Fax: +33467149119*

Abstract

In this work, silicon nanowires (SiNWs) were produced by the combination of nanosphere lithography and metal-assisted chemical etching (MACE). The SiNWs were coated with a ZnO layer by Atomic Layer Deposition (ALD). Structural properties of SiNWs/ZnO were investigated by X-ray diffraction, Raman, scanning electron microscopy and transmission electron microscopy. Optical characterizations were performed by reflectance and

photoluminescence spectroscopy. The X-ray diffraction analysis revealed that all samples have hexagonal wurtzite structure. The grain sizes are found to be in the range of 7 - 14 nm. The study of photoluminescence (PL) spectra of SiNWs/ZnO showed the domination of defect emission bands, which points to deviations of stoichiometry of the prepared 3D ZnO nanostructures. We observed also the reduction of the PL intensity of SiNWs/ZnO with the increase of Si NWs etching time corresponding to an advanced light scattering with the increase of the nanowire length.

Keywords: Silicon nanowires (SiNWs), metal-assisted chemical etching (MACE), nanosphere lithography (NSL), atomic layer deposition (ALD), ZnO

1. Introduction

Since decades, silicon (Si) continues to be the most widely used semiconductor. Such great interest in this material is due to its beneficial features as high stability and non-toxicity, quantum confinement effects, high carrier mobility and well-established fabrication technique [1]. Because of morphological and energetic features, silicon nanomaterials, are known as one of the most important types of nanomaterials. Nowadays, one dimensional (1D) silicon nanostructures, *i.e.*, silicon nanowires (SiNWs) and Si nanopillars, are of great interest because of their abilities to scatter and trap incident light, large surface to volume ratio, and other special electronic and optical properties that make possible using SiNWs as promising blocks for a range of applications including electronic devices[2-4], energy storage devices[5, 6], thermoelectrics[7-9], and biosensors[10-13].

The first preparation of Si whiskers with <111> orientation, or filamentary Si crystals with macroscopic dimensions was reported in 1957 by Treuting and coworkers [14].

Thereafter, in 1964, Wagner and Ellis performed the illuminating work and established the vapor-liquid-solid (VLS) mechanism of the Si whisker growth [15]. These pioneer studies open exciting possibilities for fabrication and investigation of SiNWs. In 2002, Peng and coworkers introduced a HF-etching-assisted nanoelectrochemical strategy to synthesize wafer-scale aligned SiNWs [16]. To date, there are many different techniques to produce silicon nanowires such as chemical vapor deposition using the VLS (Vapor—Liquid—Solid) mechanism [17], laser ablation[18], molecular beam epitaxy[19], chemical etching[20], and solution growth[21]. Among various preparation methods, the metal-assisted chemical etching (MACE) of silicon substrates in combination with nanosphere lithography (NSL) has recently emerged as a promising method to fabricate large areas of ordered SiNWs.[22, 23] The combination of MACE and NSL techniques is under increasing attention, especially because MACE is a simple and inexpensive process, which allows controlling various parameters of the etched nanostructures, such as cross-sectional shape, diameter, length, and crystallographic orientation.[24-26] The main advantages of NSL are its short preparation time, high level of hexagonal structure orientation and possibility of application of large, monolayered masks directly onto any kind of surfaces.[27-29]

Integration of SiNWs arrays as core and Zinc oxide (ZnO) as shell can have a strong impact on the development of sensing elements with improved properties. Si is an attractive substrate because of its low cost, good thermal conductivity, high crystalline quality, and availability of large size substrates with different types of conductivity (doping). In addition, silicon is the best candidate for miniaturized electronic devices and for the further development of modern nanoelectronic technology.

In parallel, ZnO is a wide bandgap (3.4 eV) semiconductor, which has a stable Wurtzite structure with lattice spacing a = 0.325 nm and c = 0.521 nm [30, 31]. It has attracted intensive research effort for its unique properties such as a thermal and chemical stability,

optical transparency, piezoelectricity, etc.[32] The attractiveness of ZnO is increased also due to its simplicity and the ease by which it can be synthesized as thin-film layer using a variety of techniques, including atomic layer deposition (ALD)[33, 34]. ALD is a special modification of chemical vapor deposition (CVD) method, capable of angstrom resolution, layer-by-layer growth of compound films.[35] The reaction between the incoming precursors and surface species is self-terminating. As a result, atomic level control of film growth can be achieved. Nowadays it is becoming a promising deposition method for growing uniform thin and ultra-thin films, especially in the cases when precise film thickness control (should be determined by the number of reaction cycles), high reproducibility, thickness uniformity and excellent conformity are required.[36]

In the present work, the silicon nanowires produced by gold-assisted chemical etching in combination with nanosphere lithography followed by ALD-based coating with ZnO layer are investigated. The structural and optical properties of the obtained nanostructures are evaluated.

2. Materials and methods

2.1.Materials

Micro particles based on polystyrene, size 1 μm, 10 wt% aqueous solution (89904), sodium dodecyl sulfate (436143), Hydrofluoric acid HF 40% (47590), Perdrogen H_2O_2 30% (31642), Nitric acid (30709), Hydrochloric acid (258148), Diethyl zinc (DEZ) ($Zn(CH_2CH,)_2$, 95% purity, CAS: 557-20-0) were purchased from Sigma Aldrich. Boron doped (8-25 Ω cm) p-type (100) crystal orientation Si wafers (LG Siltron Inc. Korea) were used as substrates.

2.2.Synthesis of SiNWs

The organized silicon nanowires were produced by gold-assisted chemical etching in combination with nanosphere lithography.[22] For this experiment, the monolayers were prepared with polystyrene particles (diameter 1 μm). The 1x1 and 2x2 cm^2 pieces of Si wafers were cleaned sequentially with deionized water (18.2 MΩ cm), ethanol and acetone by ultrasonication for 15 min in each solvent. Then the substrates were treated by O_2 plasma to have a hydrophilic surface. After the pretreatment, an ordered monolayer of polystyrene spheres (PSS) was prepared by self-assembly. The floating-transferring technique was utilized to deposit PSS on Si substrate. The polystyrene solution (40 μl) diluted by an equal amount of ethanol, was applied onto the modified substrate, which spread all over the substrate. After holding the substrate stationary for a while to obtain good dispersion of the suspension, the wafer was then slowly immersed into the glass vessel filled with deionized water and PSS started to form an unordered monolayer on the water surface. Then, one drop of 10% sodium dodecyl sulfate (SDS) solution was added to the water to change the surface tension and to consolidate the particles. The addition of SDS solution was an important step to produce 2D ordered colloidal array.[37] As a result, a large monolayer with highly ordered areas was obtained. Then this monolayer of PSS was transferred to the target substrate.

The quality of the PSS monolayer mask can be assessed right away by looking at the uniformity of the color throughout the whole area. The reflected color of the pattern varies with the size of the spheres and its quality. After the sample was dried in air at room temperature, the spheres were self-assembled into a close-packed, two-dimensional ordered lattice *via* attractive capillary forces[38, 39]. Then the diameter of spheres was decreased by O_2 plasma etching for 5 min to expose the surface of wafer for metal deposition. Plasma etching is capable of uniform and fast modification of nanospheres, and it can control the sphere diameter by adjusting the etching time.[40] In order to stick the PS spheres at the Si surface, a heat treatment at 100 °C for 30 min was performed. On the next step a thin Au film

was deposited by physical vapor deposition (PVD). The sputtering was carried out at a discharge of 25 mA in a vacuum with a pressure below 0.1 mbar. The samples covered by Au were etched with a solution consisting of $H_2O/H_2O_2/HF$ in the volume ratio 1:0.15:0.3 respectively, at room temperature for 1, 2, 5 and 7 minutes. To remove the metal, the samples where dipped in an aqua regia solution (a mixture of nitric acid and hydrochloric acid). After this, the PS spheres were etched by O_2 plasma. Figure 1 represents the overall process for the synthesis of SiNWs.

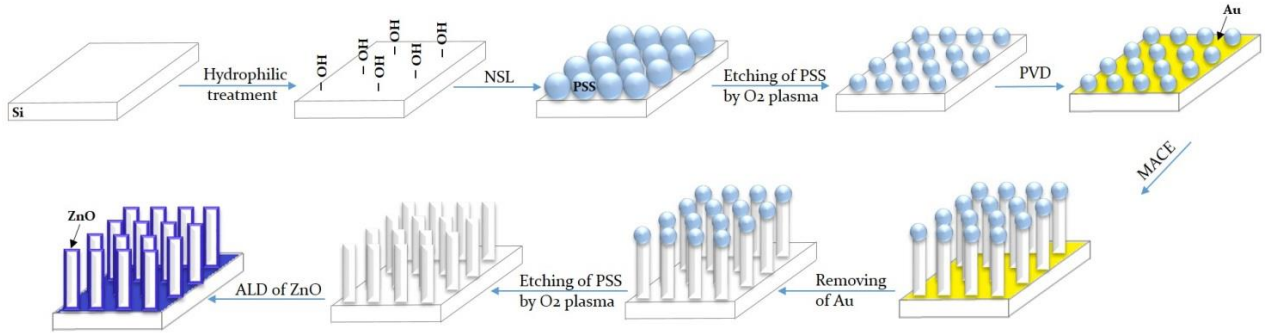

Figure 1. The schematic diagram of overall process for the synthesis of SiNWs by combining MACE and NSL techniques

The samples with organized SiNWs were then placed into the ALD chamber for the synthesis of SiNWs/ZnO coating material.

2.3.Synthesis of ZnO coating Si nanowires arrays

A custom-made ALD reactor was used for the synthesis of ultrathin ZnO films. ALD was performed using sequential exposures of DEZ and H_2O separated by a purge of Argon with a flow rate of 100 standard cubic centimeters per minute (sccm). The deposition regime for ZnO consisted of 0.2 s pulse of DEZ, 40 s of exposure to DEZ, 60 s of purge with argon followed by 2 s pulse of H_2O, 40 s of exposure to H_2O, and finally 60 s purge with argon.

Thus, 20 and 50 nm thick ZnO layers were deposited on silicon nanowires using 100 and 250 ALD cycles, respectively. The deposition was performed at 100°C. The typical growth rate for ZnO coating during these cycles is found to be 0.2 nm per cycle.

2.4.Characterization

Structural and chemical compositions of the SiNWs/ZnO were analyzed by scanning electron microscopy (SEM, S-4800, Hitachi), and the X-Ray diffraction (PANAlyticalXpert-PRO diffractometer equipped with a X'celerator detector using Ni-filtered Cu-radiation). The XRD spectra were measured in the 2θ angular region between 10° and 60°. From the latter, the grain size was calculated by the Debye-Scherer equation. SiNWs covered by ZnO ALD were investigated as well by transmission electron microscopy (TEM) (JEOL ARM 200F high-resolution transmission electron microscope (200 kV) with an EDX analyzer). The cross-sections and lamellas for TEM investigations were prepared by Focused Ion Beam (FIB) with procedures described elsewhere.[41] The FIB milling was carried out with a JEOL, JIB-4000.

Raman scattering measurements were performed using a Renishaw micro-Raman spectrometer equipped with a confocal microscope (Leica). The samples were measured in backscattering geometry with a spectral resolution of 1.0 cm^{-1}. The incident light was not polarized and also the light detector contained no polarization filters. The Raman scattering spectra were excited by a 488 nm laser. The beam was focused on the samples with a 50 x microscope objective with a numerical aperture of 0.4. The incident optical power was changed by using neutral density filters in the beam path.

Optical properties of the samples have been studied by diffuse reflectance spectroscopy (the spectral range 200-1400 nm). The diffuse reflectance spectroscopy has been performed using standard Shimadzu UV-3600 spectrophotometer with scanning step of 1 nm. Photoluminescence spectroscopy was studied in spectral range of 350−800 nm. The

measurements were performed at a standard fluorometer (FS5 Spectrofluorometer (Edinburg instruments Ltd, 2 Bain Square, Kirkton Campus, EH54 7DQ, UK)). The excitation of luminescence was performed at a wavelength of 280 nm.

3. Results and discussion

Figure 2 represents a dependence of the diameter of PSS as the function of different etching times by O_2 plasma (insets: 1 (Figure 2b), 5 (Figure 2c) and 10 min (Figure 2d)). The etching of PSS by O_2 plasma from 1 to 10 minutes allows decreasing the PSS diameter from 960±10 nm to 610±10 nm. Figure 2a demonstrates the SEM image of PS spheres deposited on Si wafer, which confirms the possibility to obtain a relatively large area, close-packed, hexagonal polystyrene monolayer, produced by floating-transferring technique. Figure 2f shows a photograph of a monolayer pattern of PSS prepared by the mentioned technique on 2x2 cm^2 silicon wafer. The color of the substrate observed in this photograph is due to the diffraction of light.

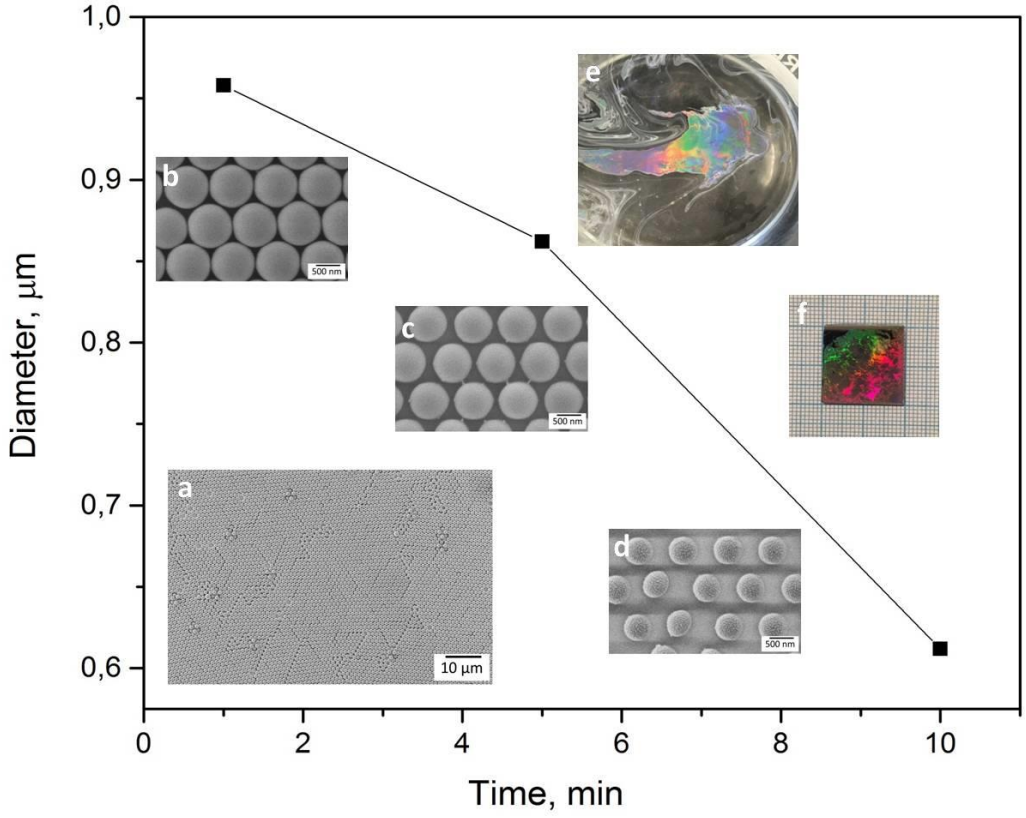

Figure 2. Diameter of PSS as the function of the O_2 plasma etching: Inset consists of SEM images of the PSS as-prepared by floating transferring technique (a) and with different O_2 plasma etching times: 1 (b), 5 (c) and 10 (d) min, respectively. Photographs of the monolayer of PSS on the water surface (e) and 2x2 cm^2 silicon wafer covered with monolayer built from 1 µm PS latex beads by the mentioned before technique (f).

Figure 3 shows the final structure of Si NWs (etching time is 5 min) after depositing 50 nm ZnO film by ALD. The SEM images indicate a conformal coating of Si substrate by ALD.

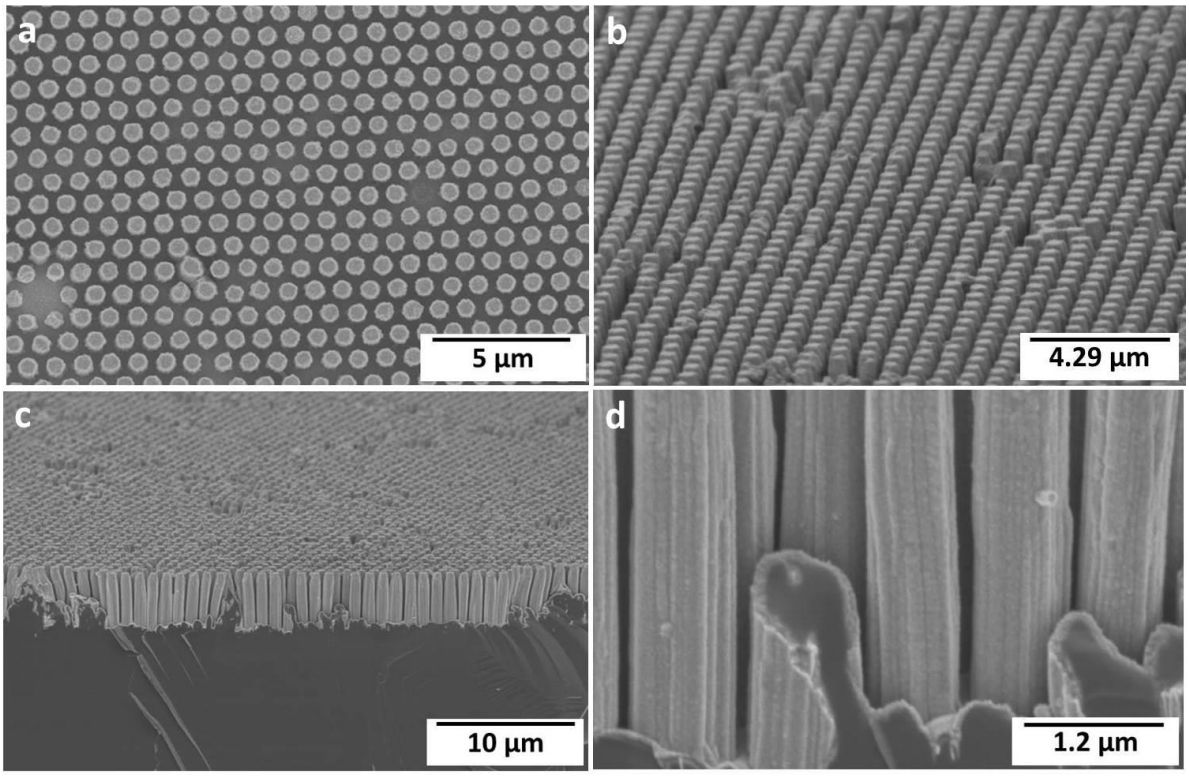

Figure 3. SEM images of SiNWs (etching time is 5 min) with 50 nm ZnO ALD layer.

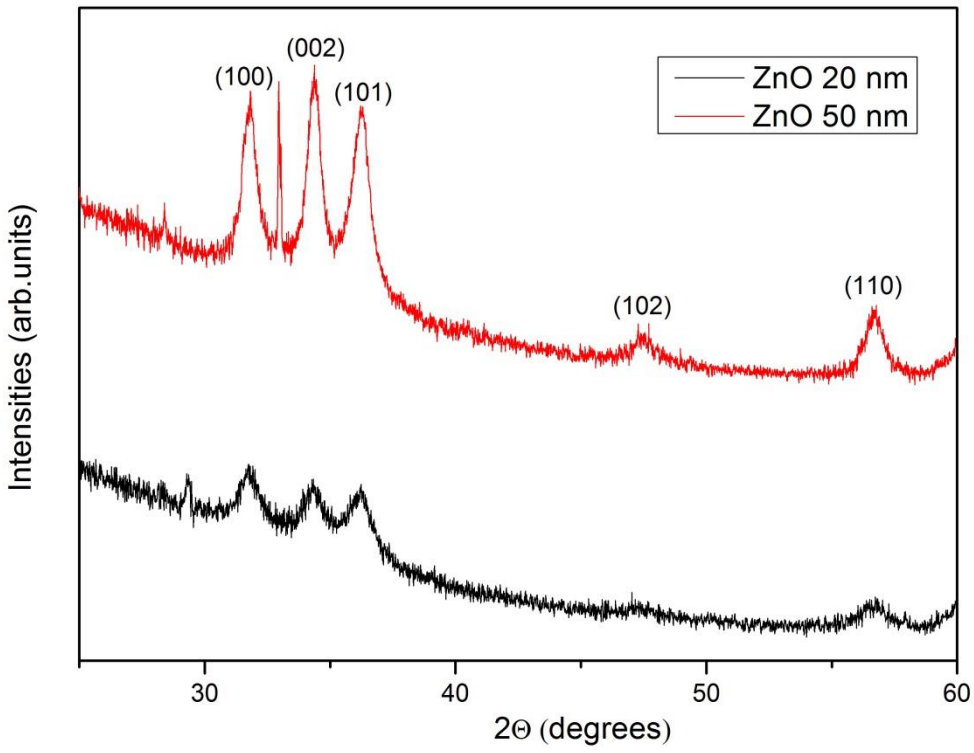

Figure 4. XRD spectra of SiNWs/ZnO with different thicknesses (20 and 50 nm) of ZnO layers on SiNWs with 7 min etching.

Figure 4 shows the XRD spectra of 20 and 50 nm ZnO films deposited on the silicon nanowires substrate with 7 minute etching. All peaks in the recorded range were identified.[33, 42, 43] The respective positions of ZnO diffraction peaks show that all the films are polycrystalline with ZnO hexagonal wurtzite structure. The XRD patterns consists of the diffraction peaks of ZnO at 2θ values of 31.78°, 34.35°, 36.25° and 56.69° attributed to (100), (002), (101) and (110) planes, that have been observed for both ZnO thickness spectra (but with rather low intensity). The increase of the ZnO thickness (50 nm) led to the appearance of XRD peaks at 2θ = 47.46° corresponding to (102) reflections of ZnO.

The grain sizes (D) of the deposited films are estimated using the following formula [34]:

$$D = \frac{0.9\lambda}{\beta \cos(\theta)}$$

where λ is the wavelength of X-ray used (λ = 0.154 nm), β is the full width at half maximum intensity in radians, and θ is the Bragg angle. The average value of grain size is found to be 7.5±0.45 nm and 14±6.5 nm for samples etched for 7 minutes and covered with 20 and 50 nm ZnO, respectively.

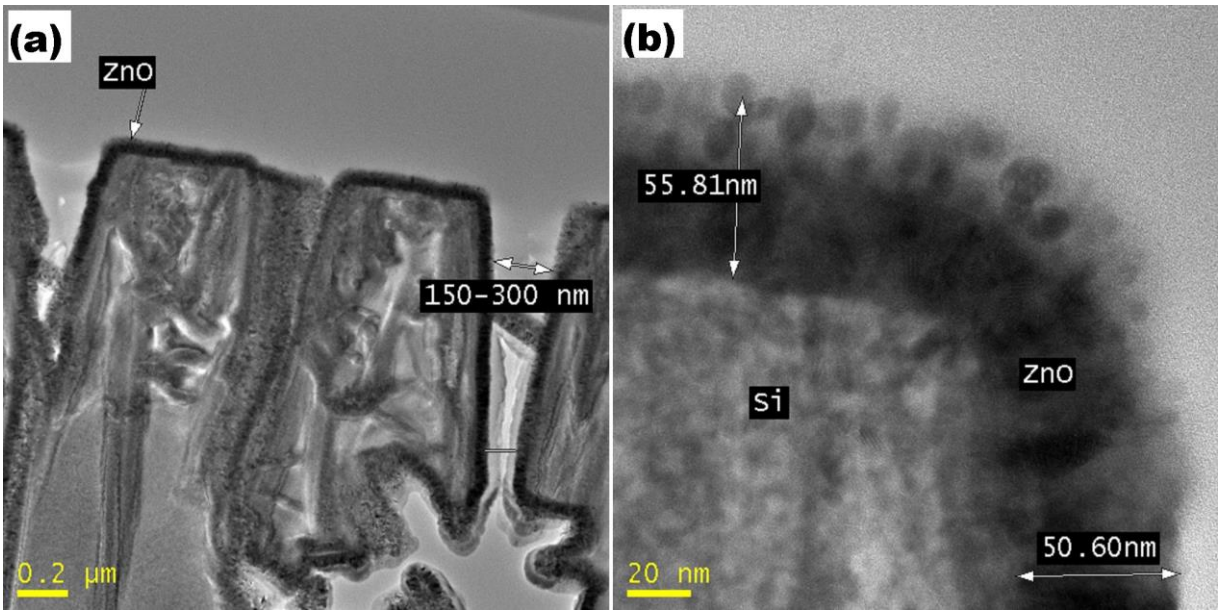

Figure 5. Cross-sectional view TEM image of ZnO-Si nanowires with different ZnO layer thicknesses: (a) 20 nm and (b) 50 nm.

Figure 5 shows the high-resolution TEM images of ZnO-Si nanowires with different ZnO layer thicknesses. Silicon nanowires coated with 20 nm of ZnO by ALD are presented in Figure 5a. ZnO coating is seen to always have a thickness of 20 nm. It is clearly seen that the distance between the nearest wires is narrowed to the bottom from 150 to 300 nm. We can notice that the diameter of the wires is about 450 nm on the top and 850 nm at the bottom. Thus, wires have the shape of a truncated trapezoid. That would come from the longer exposure time of the top part to the etching solution according to Dawood *et al.* [44]. Macroporous structure of the wires could be also observed (Fig. 5a). It can be explained by the lateral transport of the charge carriers.[22]

Figure 5b shows a TEM image of individual silicon nanowires covered by 50 nm ALD ZnO layer. The total thickness of the layer is approximately 50 nm, having the maximum value on the top (55 nm). For both samples, the ZnO layers are in a polycrystalline phase. The size of nanocrystallites was estimated using elliptical shape fitting and the longer axis was

used as the nanocrystallite size. The average grain size for 50 nm and 20 nm layer thicknesses was almost the same, 11.8±2.5 nm and 10±2.5 nm, respectively. These results confirmed the data obtained by XRD. The TEM images demonstrate the ability to produce highly uniform layers of ZnO covered silicon nanowires by the ALD-based processes.

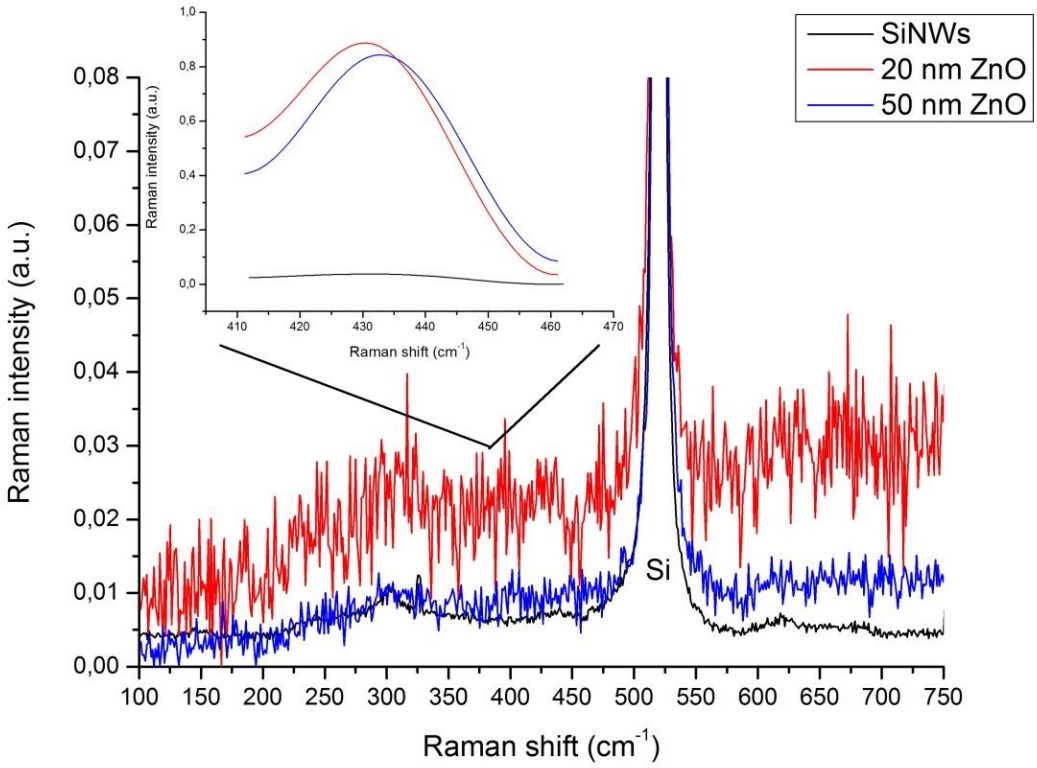

Figure 6. The Raman spectra of the Si NWs as-prepared (etching time is 7 min) and after the deposition of ZnO 20 nm and 50 nm, respectively.

In order to confirm the composition of silicon nanowires covered by ALD ZnO, Raman spectroscopy has been used. Figure 6 shows the Raman spectra of Si nanowires (7 min. etching) with 20 and 50 nm ZnO layer. Raman spectra of the as-prepared Si NWs/ZnO showed no significant peaks of ZnO in the background of the strong spectrum of the Si (520 cm^{-1}), indicating the small amount and/or the polycrystalline/amorphous phase of ZnO.

However, increasing the number of accumulations allowed us to observe the Raman peak at about 432±2 cm^{-1} (E_2^{high} mode), corresponding to the Wurzite phase of ZnO, associated with the motion of oxygen atoms (inset of Figure 6).[45-47] It is typical of the Wurzite ZnO phase, but the peak is broader (full width half maximum – FWHM, is about 20 cm^{-1}) with respect to the bulk value (FWHM is less than 10 cm^{-1}) and blue-shifted.[45-47] This broading and shifting could be explained by the quantum confinement effects in ZnO nanocrystals.[46-48]

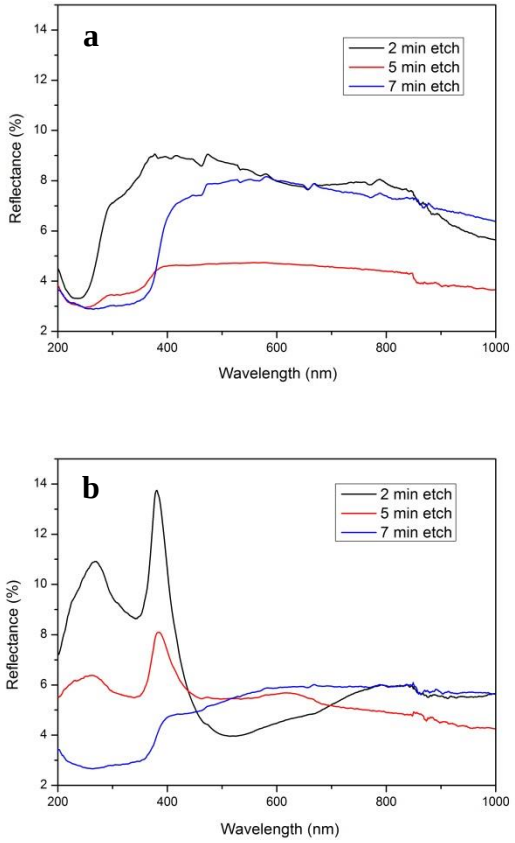

Figure 7. The reflection spectra of the SiNWs prepared at different etching times (2, 5 and 7 min) and after deposited of ZnO 20 nm (a) and 50 nm (b), respectively.

Figure 7 shows the reflectance of Si nanowires arrays etched for 2, 5 and 7 minutes and covered with 20 (a) and 50 nm (b) of ZnO, respectively. It was found that the reflectance decreases with increasing of etching time, for longer Si nanowires. This may be explained by

the more effective light trapping and more absorption of longer nanowires. We observe that the reflectance is less than 5% and 8% for the SiNWs (etching time is 5 minutes) covered with ZnO 20 and 50 nm, respectively. Such low reflectance could be explained by the energy band structure of the sample. Various band gaps in the system causes a variety of near band-edge absorption from sunlight in different frequency ranges, reducing reflectivity. Also the change of the refractive indexes of the materials may effect on the reflection reduction. [49] The optical reflectance spectra for SiNWs/ZnO presented in Figure 7 confirm the low optical reflection of thin films. Layer of ZnO on SiNWs can work as antireflection coating.

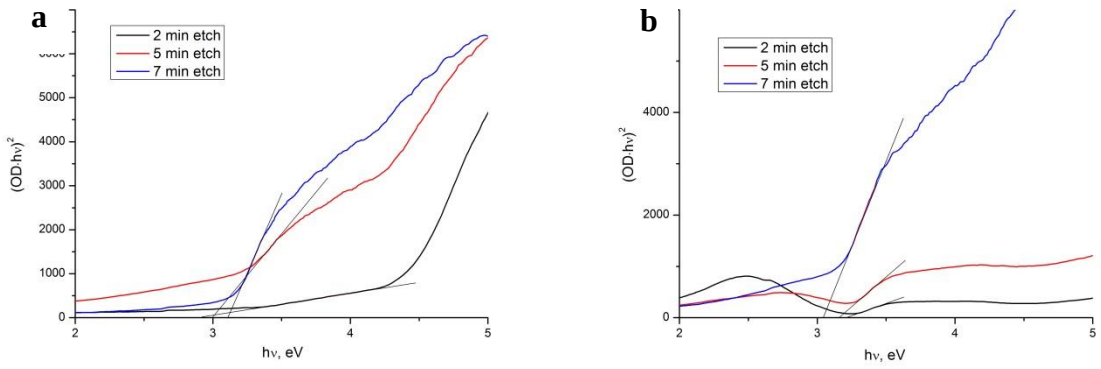

Figure 8. Band gap estimation of SiNWs covered with 20 (a) and 50 nm ZnO (b) by ALD, respectively.

Table 1. Band gap of SiNWs covered with 20 and 50 nm ZnO.

Etching time, min	2	5	7
	E_g (eV)		
ZnO 20 nm	2.90 ± 5-7 %	3.00 ± 5-7 %	3.11 ± 5-7 %
ZnO 50 nm	3.22 ± 5-7 %	3.16± 5-7 %	3.05 ± 5-7 %

The band gap values of SiNWs, prepared at different etching times (2, 5 and 7 minutes) and covered with 20 (a) and 50 nm ZnO (b) by ALD, were graphically calculated in the linear part of the absorption edge and showed in Figure 8. As we can see, the obtained values (presented in Table 1) are lower than the value typical of a ZnO single crystal (E_g = 3.37 eV). As reported before, this difference could be due to the concentration of point defects (such as vacancies and interstitials of Zn and O).[33] We can also observe a small increase of the band gap value with ZnO thickness, which could be associated with improvement of the crystalline structure of the deposited samples[33].

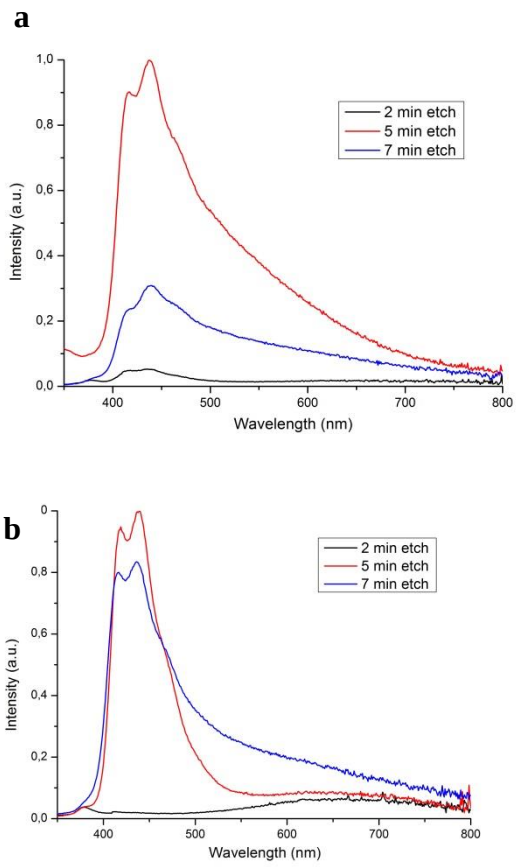

Figure 9. Photoluminescence spectra of SiNWs prepared at different etching times – 2, 5 and 7 minutes, and after ALD of 20 (a) and 50 nm ZnO (b), respectively.

PL of 3D ZnO nanostructures with different thicknesseses is plotted in Figure 9. The PL spectra showed strong peaks in the range of 410-450 nm with long PL tail to higher wavelengths. Deconvolution of the PL spectra on separate lines has been performed using Gauss fitting in Origin software (see supporting information, Figure S1). The spectra deconvolution showed peaks, centered at 376-379, 411-415, 434-437, 447-480, 490-540, 570-640 nm, 660-740 nm related to free exciton, Zn interstitials, Zn vacancies, neutral oxygen vacancies, single charged oxygen vacancies, double charged oxygen vacancies and surface defects, respectively [33, 43, 50, 51]. Domination of defect emission bands points to deviations of stoichiometry of the prepared 3D ZnO nanostructures. The decrease of PL intensity for ZnO samples, deposited on 7 min etched Si nanowires could be related to higher light scattering with the increase of the nanowire length.

4. Conclusion

In summary, we have demonstrated a simple and inexpensive method for the fabrication of ordered aligned SiNWs. The method utilizes 2D non-close-packed polystyrene sphere template for metal deposition in metal-assisted chemical etching of silicon. Here, conformal deposition of ZnO was performed on highly-ordered vertical SiNWs array by ALD technique. The ordered SiNWs readily produced by the present method may find a number of applications in array devices, such as field-effect transistors, sensors, electrodes, and two-dimensional photonic crystals. The high aspect ratio, anti-reflective characteristics inherent to nanowires structure can be exploited for fabricating future nanoelectronic and optoelectronic devices. The detailed study of structural and optical properties of core-shell SiNWs/ZnO heterostructure was represented. The X-ray diffraction analysis revealed that all samples have hexagonal Wurtzite structure. The grain sizes , as measured using XRD data, were found to be in the range of 7 - 14 nm, and confirmed by TEM measurement. The TEM and SEM images

demonstrated the ability to produce highly uniform layers of ZnO covered silicon nanowires by the ALD processes. The optical reflectance spectra for SiNWs/ZnO confirmed the low optical reflection of thin films. The layer of ZnO on SiNWs can be applied as an antireflection coating. The study of photoluminescence (PL) spectra of SiNWs/ZnO showed the domination of defect emission bands, which points to deviations of stoichiometry of the prepared 3D ZnO nanostructures. We observed also the reduction of the PL intensity of SiNWs/ZnO with the etching time for 7 minutes that could be due to the higher light scattering with the increase of the nanowire length.

5. Acknowledgment

I.I. acknowledges the financial support from the National Science Centre of Poland by the SONATA 11 project UMO-2016/21/D/ST3/00962.

6. References

[1] K.-Q. Peng, X. Wang, L. Li, Y. Hu, S.-T. Lee, Silicon nanowires for advanced energy conversion and storage, Nano Today, 8 (2013) 75-97.
[2] Y. Cui, Z. Zhong, D. Wang, W.U. Wang, C.M. Lieber, High Performance Silicon Nanowire Field Effect Transistors, Nano Letters, 3 (2003) 149-152.
[3] J. Goldberger, A.I. Hochbaum, R. Fan, P. Yang, Silicon Vertically Integrated Nanowire Field Effect Transistors, Nano Letters, 6 (2006) 973-977.
[4] L.J. Chen, Silicon nanowires: the key building block for future electronic devices, Journal of Materials Chemistry, 17 (2007) 4639-4643.
[5] L.-F. Cui, R. Ruffo, C.K. Chan, H. Peng, Y. Cui, Crystalline-Amorphous Core−Shell Silicon Nanowires for High Capacity and High Current Battery Electrodes, Nano Letters, 9 (2009) 491-495.
[6] M. Pavlenko, E.L. Coy, M. Jancelewicz, K. Zaleski, V. Smyntyna, S. Jurga, I. Iatsunskyi, Enhancement of optical and mechanical properties of Si nanopillars by ALD TiO2 coating, RSC Advances, 6 (2016) 97070-97076.
[7] A.I. Hochbaum, R. Chen, R.D. Delgado, W. Liang, E.C. Garnett, M. Najarian, A. Majumdar, P. Yang, Enhanced thermoelectric performance of rough silicon nanowires, Nature, 451 (2008) 163-167.
[8] A.R. Abramson, K. Woo Chul, S.T. Huxtable, Y. Haoquan, W. Yiying, A. Majumdar, T. Chang-Lin, Y. Peidong, Fabrication and characterization of a nanowire/polymer-based nanocomposite for a prototype thermoelectric device, Journal of Microelectromechanical Systems, 13 (2004) 505-513.

[9] A.I. Boukai, Y. Bunimovich, J. Tahir-Kheli, J.-K. Yu, W.A. Goddard Iii, J.R. Heath, Silicon nanowires as efficient thermoelectric materials, Nature, 451 (2008) 168-171.
[10] Y. Cui, Q. Wei, H. Park, C.M. Lieber, Nanowire Nanosensors for Highly Sensitive and Selective Detection of Biological and Chemical Species, Science, 293 (2001) 1289-1292.
[11] D.R. Kim, X. Zheng, Numerical characterization and optimization of the microfluidics for nanowire biosensors, Nano Letters, 8 (2008) 3233-3237.
[12] F. Patolsky, G. Zheng, C.M. Lieber, Nanowire-Based Biosensors, Analytical Chemistry, 78 (2006) 4260-4269.
[13] T.-E. Bae, H.-J. Jang, J.-H. Yang, W.-J. Cho, High Performance of Silicon Nanowire-Based Biosensors using a High-k Stacked Sensing Thin Film, ACS applied materials & interfaces, 5 (2013) 5214-5218.
[14] R. Treuting, S. Arnold, Orientation habits of metal whiskers, Acta Metallurgica, 5 (1957) 598.
[15] R.S. Wagner, W.C. Ellis, VAPOR-LIQUID-SOLID MECHANISM OF SINGLE CRYSTAL GROWTH, Applied Physics Letters, 4 (1964) 89-90.
[16] K.-Q. Peng, Y.-J. Yan, S.-P. Gao, J. Zhu, Synthesis of large-area silicon nanowire arrays via self-assembling nanoelectrochemistry, Advanced materials, 14 (2002) 1164.
[17] D. Lerose, M. Bechelany, L. Philippe, J. Michler, S. Christiansen, Ordered arrays of epitaxial silicon nanowires produced by nanosphere lithography and chemical vapor deposition, Journal of Crystal Growth, 312 (2010) 2887-2891.
[18] N. Fukata, T. Oshima, T. Tsurui, S. Ito, K. Murakami, Synthesis of silicon nanowires using laser ablation method and their manipulation by electron beam, Science and Technology of Advanced Materials, 6 (2005) 628-632.
[19] B. Fuhrmann, H.S. Leipner, H.-R. Höche, L. Schubert, P. Werner, U. Gösele, Ordered Arrays of Silicon Nanowires Produced by Nanosphere Lithography and Molecular Beam Epitaxy, Nano Letters, 5 (2005) 2524-2527.
[20] Y.J. Zhang, W. Li, K.J. Chen, Application of two-dimensional polystyrene arrays in the fabrication of ordered silicon pillars, Journal of Alloys and Compounds, 450 (2008) 512-516.
[21] N.-M. Park, C.-J. Choi, Growth of silicon nanowires in aqueous solution under atmospheric pressure, Nano Research, 7 (2014) 898-902.
[22] B. Mikhael, B. Elise, M. Xavier, S. Sebastian, M. Johann, P. Laetitia, New silicon architectures by gold-assisted chemical etching, ACS applied materials & interfaces, 3 (2011) 3866-3873.
[23] M. Pavlenko, E. Coy, M. Jancelewicz, K. Załęski, V. Smyntyna, S. Jurga, I. Iatsunskyi, Enhancement of optical and mechanical properties of Si nanopillars by ALD TiO 2 coating, RSC Advances, 6 (2016) 97070-97076.
[24] Z. Huang, N. Geyer, P. Werner, J. De Boor, U. Gösele, Metal-assisted chemical etching of silicon: a review, Advanced materials, 23 (2011) 285-308.
[25] H. Han, Z. Huang, W. Lee, Metal-assisted chemical etching of silicon and nanotechnology applications, Nano Today, 9 (2014) 271-304.
[26] N. Geyer, N. Wollschläger, B. Fuhrmann, A. Tonkikh, A. Berger, P. Werner, M. Jungmann, R. Krause-Rehberg, H.S. Leipner, Influence of the doping level on the porosity of silicon nanowires prepared by metal-assisted chemical etching, Nanotechnology, 26 (2015) 245301.
[27] J. Rybczynski, M. Hilgendorff, M. Giersig, Nanosphere lithography—Fabrication of various periodic magnetic particle arrays using versatile nanosphere masks, in: Low-Dimensional Systems: Theory, Preparation, and Some Applications, Springer, 2003, pp. 163-172.
[28] P. Colson, C. Henrist, R. Cloots, Nanosphere lithography: a powerful method for the controlled manufacturing of nanomaterials, Journal of Nanomaterials, 2013 (2013) 21.
[29] E.M. AKINOGLU, A.J. MORFA, M. GIERSIG, Nanosphere lithography-exploiting self-assembly on the nanoscale for sophisticated nanostructure fabrication, Turkish Journal of Physics, 38 (2014) 563-572.
[30] M. Bechelany, A. Amin, A. Brioude, D. Cornu, P. Miele, ZnO nanotubes by template-assisted sol–gel route, Journal of Nanoparticle Research, 14 (2012) 1-7.

[31] E. Robak, E. Coy, M. Kotkowiak, S. Jurga, K. Zaleski, H. Drozdowski, The effect of Cu doping on the mechanical and optical properties of zinc oxide nanowires synthesized by hydrothermal route, Nanotechnology, 27 (2016).
[32] Ü. Özgür, Y.I. Alivov, C. Liu, A. Teke, M.A. Reshchikov, S. Doğan, V. Avrutin, S.-J. Cho, H. Morkoç, A comprehensive review of ZnO materials and devices, Journal of Applied Physics, 98 (2005) 041301.
[33] A.A. Chaaya, R. Viter, M. Bechelany, Z. Alute, D. Erts, A. Zalesskaya, K. Kovalevskis, V. Rouessac, V. Smyntyna, P. Miele, Evolution of microstructure and related optical properties of ZnO grown by atomic layer deposition, Beilstein Journal of Nanotechnology, 4 (2013) 690-698.
[34] V. Roman, C. Adib Abou, I. Igor, N. Grzegorz, K. Kristaps, E. Donats, M. Philippe, S. Valentyn, B. Mikhael, Tuning of ZnO 1D nanostructures by atomic layer deposition and electrospinning for optical gas sensor applications, Nanotechnology, 26 (2015) 105501.
[35] C. Marichy, M. Bechelany, N. Pinna, Atomic Layer Deposition of Nanostructured Materials for Energy and Environmental Applications, Advanced materials, 24 (2012) 1017-1032.
[36] I. Iatsunskyi, M. Jancelewicz, G. Nowaczyk, M. Kempiński, B. Peplińska, M. Jarek, K. Załęski, S. Jurga, V. Smyntyna, Atomic layer deposition TiO 2 coated porous silicon surface: Structural characterization and morphological features, Thin Solid Films, 589 (2015) 303-308.
[37] Y. Zhang, X. Wang, Y. Wang, H. Liu, J. Yang, Ordered nanostructures array fabricated by nanosphere lithography, Journal of Alloys and Compounds, 452 (2008) 473-477.
[38] P.A. Kralchevsky, K. Nagayama, Capillary forces between colloidal particles, Langmuir, 10 (1994) 23-36.
[39] K.D. Danov, B. Pouligny, P.A. Kralchevsky, Capillary Forces between Colloidal Particles Confined in a Liquid Film: The Finite-Meniscus Problem, Langmuir, 17 (2001) 6599-6609.
[40] S.S. Shinde, S. Park, Oriented colloidal-crystal thin films of polystyrene spheres via spin coating, Journal of Semiconductors, 36 (2015) 023001.
[41] I. Iatsunskyi, E. Coy, R. Viter, G. Nowaczyk, M. Jancelewicz, I. Baleviciute, K. Załęski, S. Jurga, Study on Structural, Mechanical, and Optical Properties of Al2O3–TiO2 Nanolaminates Prepared by Atomic Layer Deposition, The Journal of Physical Chemistry C, 119 (2015) 20591-20599.
[42] A.A. Chaaya, R. Viter, I. Baleviciute, M. Bechelany, A. Ramanavicius, D. Erts, V. Smyntyna, P. Miele, Optical and structural properties of Al2O3/ZnO nanolaminates deposited by ALD method, Physica status solidi (c), 11 (2014) 1505-1508.
[43] A.A. Chaaya, R. Viter, I. Baleviciute, M. Bechelany, A. Ramanavicius, Z. Gertnere, D. Erts, V. Smyntyna, P. Miele, Tuning Optical Properties of Al2O3/ZnO Nanolaminates Synthesized by Atomic Layer Deposition, The Journal of Physical Chemistry C, 118 (2014) 3811-3819.
[44] M. Dawood, T. Liew, P. Lianto, M. Hong, S. Tripathy, J. Thong, W. Choi, Interference lithographically defined and catalytically etched, large-area silicon nanocones from nanowires, Nanotechnology, 21 (2010) 205305.
[45] B. Pal, P.K. Giri, Defect Mediated Magnetic Interaction and High T c Ferromagnetism in Co Doped ZnO Nanoparticles, Journal of Nanoscience and Nanotechnology, 11 (2011) 9167-9174.
[46] G. Mohan Kumar, P. Ilanchezhiyan, J. Kawakita, M. Subramanian, R. Jayavel, Magnetic and optical property studies on controlled low-temperature fabricated one-dimensional Cr doped ZnO nanorods, CrystEngComm, 12 (2010) 1887-1892.
[47] S. Kuriakose, B. Satpati, S. Mohapatra, Enhanced photocatalytic activity of Co doped ZnO nanodisks and nanorods prepared by a facile wet chemical method, Physical Chemistry Chemical Physics, 16 (2014) 12741-12749.
[48] I. Iatsunskyi, G. Nowaczyk, S. Jurga, V. Fedorenko, M. Pavlenko, V. Smyntyna, One and two-phonon Raman scattering from nanostructured silicon, Optik - International Journal for Light and Electron Optics, 126 (2015) 1650-1655.
[49] Q. Yang, D. Li, B. Yu, S. Huang, J. Wang, S. Li, J. Kang, Size effect on morphology and optical properties of branched ZnO/Si nanowire arrays, Physics Letters A, 380 (2016) 1044-1048.
[50] R. Viter, Z. Balevicius, A.A. Chaaya, I. Baleviciute, S. Tumenas, L. Mikoliunaite, A. Ramanavicius, Z. Gertnere, A. Zalesska, V. Vataman, The influence of localized plasmons on the optical properties of Au/ZnO nanostructures, Journal of Materials Chemistry C, 3 (2015) 6815-6821.

[51] R. Viter, I. Iatsunskyi, V. Fedorenko, S. Tumenas, Z. Balevicius, A. Ramanavicius, S. Balme, M. Kempiński, G. Nowaczyk, S. Jurga, Enhancement of electronic and optical properties of ZnO/Al2O3 nanolaminate coated electrospun nanofibers, The Journal of Physical Chemistry C, 120 (2016) 5124-5132.